Polarization-resolved phonon-assisted optical transitions of bound excitons in wurtzite GaN

A. A. Toropov, Yu. E. Kitaev, and T. V. Shubina
Ioffe Physico-Technical Institute, Russian Academy of Sciences, Politekhnicheskaya 26, 194021 St. Petersburg, Russia

P. P. Paskov, J. P. Bergman, and B. Monemar
Department of Physics, Chemistry and Biology, Linköping University, S-581 83 Linköping, Sweden

A. Usui
R&D Division, Furukawa Co., Ltd. Tsukuba, Ibaraki 305-0856, Japan

(Received 20 July 2007; revised manuscript received 21 January 2008; published 2 May 2008)

The selection rules of phonon-assisted optical transitions of bound excitons in bulk wurtzite GaN are studied both experimentally and theoretically. The linearly polarized photoluminescence is detected within the phonon replicas of the lines of impurity bound excitons in the geometry, when the light wave vector is normal to the hexagonal axis, and the electric field vector is either perpendicular or parallel to it. The degree and even sign of the linear polarization is found to depend on the symmetry of the involved optical phonon. To explain these data, a group-theory approach is applied to derive the selection rules for zero-phonon and phonon-assisted transitions involving excitons bound to either substitutional (C_{3v} symmetry) or interstitial (C_{3v}, C_s, or C_1 symmetries) impurities. The obtained theoretical selection rules are in an agreement with the experimental results, provided the exciton is bound to the impurities with the C_{3v} symmetry.

DOI: 10.1103/PhysRevB.77.195201 PACS number(s): 71.35.−y, 63.20.kk, 78.55.Cr

I. INTRODUCTION

Polarization-resolved optical spectroscopic techniques have long been used for the investigation of the symmetry properties of semiconductor crystals. In particular, the measurements of the linearly polarized absorption, reflectance, and photoluminescence (PL) in the region of free excitons provided many useful data about intrinsic anisotropy of the electronic system in wurtzite crystals with the uniaxial C_{6v}^4 ($P6_3mc$) symmetry. These studies allowed one to establish the order of the valence-band states in wurtzite GaN (Ref. 1) and ZnO (Ref. 2) as well as to elucidate the effects of spatial dispersion on the excitonic properties of wurtzite CdS.[3] On the other hand, only a few data were published on the polarization-resolved luminescence of impurity-bound excitons and their optical-phonon replica.[1]

In principle, these studies could supply important information about the local position and vibrations of the impurity atoms in the crystal since the respective optical selection rules depend on the symmetry of the site occupied by the impurity and on the symmetry of the involved phonon.[4–6] The polarization of the spectra measured by Dingle *et al.*[1] in bulk GaN crystals was, however, averaged over different kinds of excitons, impurities, and phonons due to the relatively large width of the PL lines (~5 meV) in the studied samples so that the information relevant to some specific donors and phonons could not be extracted. More recent papers have reported on polarization-resolved measurements of the spectrally resolved emission lines of donor-bound excitons of *A* and *B* series in better-quality wurtzite GaN.[7] Nevertheless, to the best of our knowledge, no systematic data on the linear polarization of the phonon-assisted transitions of bound excitons in wurtzite crystals have ever been published.

In this work, we study the polarization-resolved spectra of the phonon-assisted emission of bound excitons in a high-quality bulk GaN sample. The typical PL linewidth of the zero-phonon lines was as small as ~0.5 meV that allowed us to resolve the peaks relevant to individual excitons, impurities, and phonons. In terms of the site symmetry approach (see Ref. 8), we derive the selection rules for the phonon-assisted transitions of bound excitons, involving optical phonons of different symmetries and impurity atoms occupying different positions in the wurtzite crystal. On the basis of the comparison between the selection rules and the experimental data, we explain the observed anisotropy of the PL spectrum and get insight into site symmetry of the positions occupied by the impurity atoms.

The paper is organized as follows. Section II describes the experimental details and results. Section III presents our group-theory approach to the calculation of the polarization selection rules. In Sec. IV, we discuss the correspondence between the theoretical selection rules and experimental data. Finally, Sec. V concludes the paper.

II. EXPERIMENT

The studied sample was a 1-mm-thick freestanding wurtzite GaN film grown by hydride vapor phase epitaxy. The hexagonal axis was perpendicularly oriented to the plane of the film. The total residual donor concentration in this sample was estimated as 8×10^{15} cm^{-3}. The PL spectra were measured for all three essentially different polarization geometries possible in a wurtzite crystal—α polarization ($\mathbf{E}\perp\mathbf{c}$, $\mathbf{k}\|\mathbf{c}$), σ polarization ($\mathbf{E}\perp c$, $\mathbf{k}\perp\mathbf{c}$), and π polarization ($\mathbf{E}\|\mathbf{c}$, $\mathbf{k}\perp\mathbf{c}$). Here, $\mathbf{E}$ and $\mathbf{k}$ are the electric field vector and wave vector of light, while $\mathbf{c}$ denotes the hexagonal axis of the crystal. In this paper, we focus on the results obtained for the σ and π polarization geometries. These data were obtained by breaking the film and choosing for the measure-

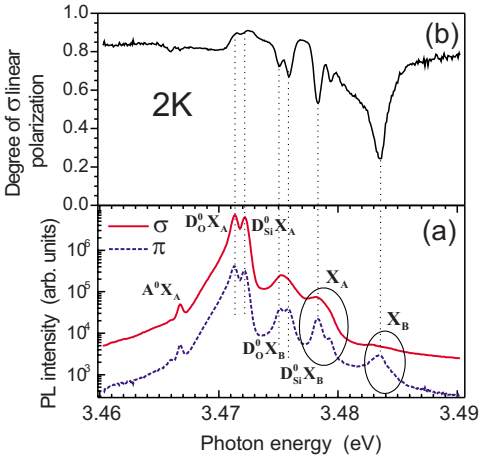

FIG. 1. (Color online) (a) Zero-phonon cw PL spectra of free and bound excitons, which are measured for σ and π polarizations. (b) The degree of σ linear polarization.

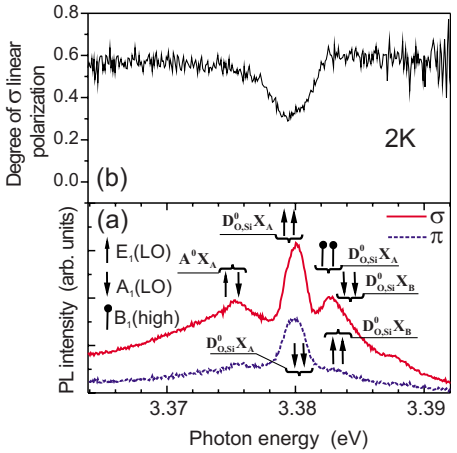

FIG. 2. (Color online) (a) 1LO-phonon replicas of bound excitons, which are measured for σ and π polarizations. The vertical lines with attached different labels point to the energies that are obtained by subtracting the excitation energy of some optical phonon from the energy of the donor-bound exciton. The correspondence between the type of phonon and the shape of the label is shown in the figure. (b) The degree of σ linear polarization.

ments flat areas of the cleaved sample edge. Stationary PL spectra were excited with the fourth harmonic of a cw Nd-:vanadate laser ($\lambda = 266$ nm) and detected with a UV-enhanced charge coupled device. The triple-frequency emission from a Ti:sapphire femtosecond pulse laser ($\lambda \sim 260$ nm) was used for transient PL measurements. The PL transients were detected by a UV sensitive Hamamatsu streak camera system with a temporal resolution better than 20 ps. In the framework of this study, the measurements of time-resolved PL were useful to identify the origin of the observed phonon-assisted emission bands. All measurements were performed at 1.9 K.

Figure 1(a) shows the σ- and π-polarized cw PL spectra measured in the region of zero-phonon lines of free and bound excitons. The dominant feature in the spectrum is a close doublet of lines at 3.471–3.472 eV ($D_O^0X^A$ and $D_{Si}^0X^A$), which is attributed to the emission of the lowest energy exciton of the A series (A exciton), bound to a neutral donor, either oxygen or silicon.[9] The respective band of free A-exciton-polaritons (X^A) emerges 6–7 meV above at 3.478–3.479 eV. The higher-energy exciton of the B series (B exciton) manifests itself as two lines of donor-bound excitons at 3.475–3.476 eV ($D_O^0X^B$ and $D_{Si}^0X^B$) and the band of free B-exciton polaritons at 3.483–3.484 eV. The weak line observed at 3.467 eV (A^0X^A) is usually attributed to A-excitons bound to a neutral acceptor.[9] Note that the lines relevant to A excitons at low temperature are 1–2 orders of magnitude stronger than the respective lines of B excitons. This is apparently due to the efficient energy relaxation of the excitons, which is accompanied by conversion of the exciton type. Fast trapping of free excitons by neutral donors as well as surface recombination are mostly responsible for the weakness of the free-exciton lines compared to the lines of the bound excitons. Figure 1(b) shows the spectrum of the degree of linear polarization. Here, positive sign corresponds to σ polarization. The polarization degree of various lines is essentially different. The detailed discussion of this spectrum is presented later in the paper after deriving the theoretical selection rules.

Figure 2(a) demonstrates the linearly polarized cw PL spectra in the region of 1LO-phonon replicas about 90 meV below the zero-phonon PL lines. Different labels in the figure point to the energies, which are obtained after subtracting the excitation energy of LO phonons (A_1 and E_1) or a silent B_1 (high) optical phonon from the energy of various zero-phonon lines of impurity-bound excitons. The notations and the values of excitation energy for optical phonons are taken as in Ref. 10. One can conclude from Fig. 2(a) that the relatively wide strong peak at 3.38 eV is a superposition of phonon replicas involving donor bound A excitons ($D_O^0X^A$ and $D_{Si}^0X^A$) as well as A_1 and E_1 LO phonons. The line at 3.375 eV perfectly fits the energies of the A_1 and E_1 LO-phonon replicas of the A^0X^A line. The third PL line emerging near 3.383 eV reasonably fits the energies of the A_1 and E_1 LO-phonon replicas of the donor bound B excitons ($D_O^0X^B$ and $D_{Si}^0X^B$) as well as the energy of the B_1(high) phonon replica of the donor-bound A excitons. The choice can be made on the basis of the measured PL transients. Indeed, the characteristic PL decay time constant for the zero-phonon line of bound B excitons (~ 120 ps) is much smaller than that of bound A excitons (~ 1100–1400 ps). The decay time constant within all three lines in Fig. 2(a) falls in the latter range, and hence, one can reliably exclude any noticeable contribution from the phonon replica of the B-bound excitons. One can see from Fig. 2(b) that all these lines are effectively σ polarized, while the polarization degree varies along the spectrum.

The PL spectrum of the replicas involving TO A_1 and E_1 phonons and a nonpolar E_2(high) optical phonon fits the region about 70 meV below the respective zero-phonon lines [see Fig. 3(a)]. While these replicas are noticeably weaker than the replicas involving LO phonons, they can be reliably detected. On the basis of the calculated energies of the possible phonon replicas and measured PL transients, we attribute the four narrow lines visible in Fig. 3(a) in the range of 3.400–3.403 eV to the replicas of the two donor-bound A excitons, involving an E_1(TO) phonon and an E_2(high) pho-

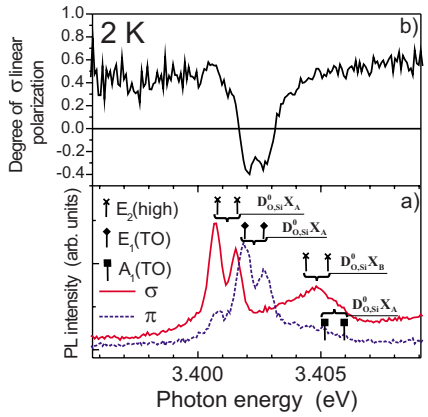

FIG. 3. (Color online) (a) One-phonon replicas of bound excitons, which are measured at σ and π polarizations for TO-phonons and an E_2(high) phonon. The vertical lines with attached different labels point to the energies that are obtained by subtracting the excitation energy of some optical phonon from the energy of the donor-bound exciton. The correspondence between the type of phonon and the shape of the label is shown in the figure. (b) The degree of σ linear polarization.

non. One can see in Figs. 3(a) and 3(b) that the replicas assisted by the E_2(high) phonon are σ polarized, whereas the E_1(TO) phonon replicas are π polarized. The identification of the relatively wide weak σ-polarized line around 3.405 meV is not so clear. Its energy position better fits the calculated energies of the E_2(high)-phonon-assisted replicas of the two donor-bound B excitons, while the PL transients rather evidence in favor of the A_1(TO) phonon replicas of the donor-bound A excitons.

Finalizing the experimental section, we comment on the issue of the accuracy of measuring the degree of linear polarization of different emission lines, as shown in Figs. 1–3. The inaccuracy mainly emerges from the existence of a linearly polarized background emission superimposed with the sharp excitonic peaks. This background is real, is spectral dependent, and has different origin in different parts of the spectrum. Therefore, it is difficult to subtract or normalize this spectral component. Note, however, that the background emission is relatively weak as compared to the peaks of our interest. The respective error of measuring the polarization degree is less then 1% for the region of zero-phonon lines of donor-bound excitons (Fig. 1) and is in the range of a few percent for their phonon replica (Figs. 2 and 3). In all cases, the degree of σ polarization of the sharp peaks is overestimated since the background is always σ polarized. This error does not noticeably influence the qualitative conclusions made in Secs. IV and V.

III. THEORY

Let us now derive, in terms of site symmetry, the selection rules for zero-phonon and phonon-assisted transitions involving excitons bound to either substitutional or interstitial impurities. In this discussion, the notation for space-group irreducible representations (irreps) follows Ref. 11, while that of point-group irreps follows Ref. 12. The description of the C_{6v}^4 ($P6_3mc$) space group and its Wyckoff positions is chosen in correspondence with Ref. 13. It should be noted that the Γ_5 and Γ_6 irreps are permuted with respect to Ref. 11 in a number of papers devoted to wurtzite structures.

For bound excitons, the states of a free exciton transform into the states, which are obtained by a subduction of the irrep describing the free exciton symmetry D_α^{exc} on the site symmetry group $G_\mathbf{q}$ of the impurity ($D_\alpha^{exc}\downarrow G_\mathbf{q}$), and the selection rules for dipole-allowed transitions are given by

$$(D_\alpha^{exc}\downarrow G_\mathbf{q}) \cap d_v \neq 0, \tag{1}$$

where d_v is the vector representation of the site symmetry group $G_\mathbf{q}$ of the impurity (see e.g., Refs. 5 and 6).

For the phonon-assisted optical transitions of bound excitons, the recombination process occurs via a virtual state d^{virt}, whereas the final state of exciton after recombination d^f is described by the unit representation d_1 of the site symmetry group $G_\mathbf{q}$. One can consider that the transition from the initial exciton state $d_\alpha^i = D_\alpha^{exc}\downarrow G_\mathbf{q}$ to a virtual state involves the phonon $d_\beta^{ph} = D_\beta^{ph}\downarrow G_\mathbf{q}$, where the irrep D_β^{ph} represents the symmetry of the phonon, whereas the transition from the virtual state to the final one involves the photon d_v. Note that in our case the irreps d_β^{ph} of phonons transform according to the vector representation like those of the photon, and hence, the phonon and the photon can be interchanged within a given process. As a result, for the phonon-assisted optical transitions of the bound excitons, the selection rules derived in Ref. 6 for the general case as

$$d^i \times d^{ph} \times (d^{virt})^* \supset d_1, \tag{2a}$$

$$(d^{virt})^* \times d_v \times d^f \supset d_1 \tag{2b}$$

can be rewritten as

$$(D_\alpha^{exc}\downarrow G_\mathbf{q}) \times (D_\beta^{ph}\downarrow G_\mathbf{q}) \cap d_v \neq 0. \tag{3}$$

In general, all excitons and phonons from the entire Brillouin zone, which after reduction transform into corresponding localized states, could participate in the processes. However, the main contribution to the emission spectra give Γ-point free excitons and $\mathbf{k}=0$ phonons, and hence, we restrict our analysis to this situation. The impurity field acting as a perturbation transforms free exciton and phonon states into the localized ones corresponding to the irreps of the site symmetry point group. One should note that this treatment would be invalid if the perturbation were strong enough to destroy the electron-hole complex.

In hexagonal GaN, the substitutional impurities and vacancies can occupy sites with C_{3v} symmetry (the $2b$ Wyckoff position), whereas interstitial impurities and molecular defects can occupy sites with C_{3v} ($2a$ and $2b$), C_s ($6c$), and C_1 ($12d$) symmetries. The $2a$ $\{(0,0,z),(0,0,z+1/2)\}$, and $2b$ $\{(1/3,2/3,z),(2/3,1/3,z+1/2)\}$ Wyckoff positions are symmetry lines rather than isolated symmetry points: the $2a$ symmetry line coincides with the sixfold screw axis (z axis), whereas the $2b$ positions form a pair of symmetry lines parallel to the sixfold screw axis, with Ga and N atoms at the $2b$ positions occupying sites with $z=0$ and $z=0.377$, respectively. The $6c$ positions are six vertical symmetry planes

TABLE I. Selection rules for the optical transitions of free and bound excitons, including the phonon-assisted transitions of bound excitons.

	A excitons		*B* excitons		
Free exciton	Γ_5	$\Gamma_6(x,y)$	$\Gamma_1(z)$	Γ_2	$\Gamma_6(x,y)$
Exciton bound to C_{3v} impurity	$e(x,y)$	$e(x,y)$	$a_1(z)$	a_2	$e(x,y)$
A_1, B_1-phonon assisted	$e(x,y)$	$e(x,y)$	$a_1(z)$	a_2	$e(x,y)$
E_1, E_2-phonon assisted	$a_1(z)+a_2$ $+e(x,y)$	$a_1(z)+a_2$ $+e(x,y)$	$e(x,y)$	$e(x,y)$	$a_1(z)+a_2$ $+e(x,y)$
Exciton bound to C_s impurity	$a'(x,y,z)$ $+a''(x,y)$	$a'(x,y,z)$ $+a''(x,y)$	$a'(x,y,z)$	$a''(x,y)$	$a'(x,y,z)$ $+a''(x,y)$
A_1, B_1-phonon assisted	$a'(x,y,z)$ $+a''(x,y)$	$a'(x,y,z)$ $+a''(x,y)$	$a'(x,y,z)$	$a''(x,y)$	$a'(x,y,z)$ $+a''(x,y)$
E_1, E_2-phonon assisted	$2a'(x,y,z)$ $+2a''(x,y)$	$2a'(x,y,z)$ $+2a''(x,y)$	$a'(x,y,z)$ $+a''(x,y)$	$a'(x,y,z)$ $+a''(x,y)$	$2a'(x,y,z)$ $+2a''(x,y)$

$\{(x,-x,z)$, $(x,2x,z)$, $(-2x,-x,z)$, $(-x,x,z+1/2)$, $(-x,-2x,z+1/2)$, $(2x,x,z+1/2)\}$ and $12d$ positions $\{(x,y,z)$, $(-y,x-y,z)$, $(-x+y,-x,z)$, $(-x,-y,z+1/2)$, $(y,-x+y,z+1/2)$, $(x-y,x,z+1/2)$, $(-y,-x,z)$, $(-x+y,y,z)$, $(x,x-y,z)$, $(y,x,z+1/2)$, $(x-y,-y,z+1/2)$, $(-x,-x+y,z+1/2)\}$ occupy the rest of the space. Here, the z direction corresponds to the hexagonal axis of the wurtzite crystal, and the angle between the x and y axes is 120°.

For free A excitons in wurtzite GaN, $D_A^{exc}=\Gamma_5+\Gamma_6(x,y)$, whereas that for free B excitons is $D_B^{exc}=\Gamma_1(z)+\Gamma_2+\Gamma_6(x,y)$ (see, e.g., Refs. 1, 14, and 15). Implementing the operation of subduction, we calculate the symmetries of the bound excitons. As a result, for $G_{\mathbf{q}}=C_{3v}$ ($\mathbf{q}=2a$ or $\mathbf{q}=2b$), we have

$$\Gamma_1\downarrow G_{\mathbf{q}}=a_1, \tag{4a}$$

$$\Gamma_2\downarrow G_{\mathbf{q}}=a_2, \tag{4b}$$

$$\Gamma_5,\Gamma_6\downarrow G_{\mathbf{q}}=e, \tag{4c}$$

with the vector representation given by $d_v=a_1(z)+e(x,y)$. Here, a_1, a_2, and e are the irreps of the C_{3v} point group. For $G_{\mathbf{q}}=C_s$ ($\mathbf{q}=6c$), we obtain

$$\Gamma_1\downarrow G_{\mathbf{q}}=a', \tag{5a}$$

$$\Gamma_2\downarrow G_{\mathbf{q}}=a'', \tag{5b}$$

$$\Gamma_5,\Gamma_6\downarrow G_{\mathbf{q}}=a'+a'', \tag{5c}$$

with the vector representation given by $d_v=a'(x,y,z)+a''(x,y)$, when many impurities are assumed to be randomly distributed over the six symmetry planes.[4] In this case, the x and y polarizations are indistinguishable. a' and a'' are the irreps of the C_s point group.

The set of optical phonons in GaN is given by $\Gamma_{opt}=\Gamma_1+2\Gamma_4+2\Gamma_5+\Gamma_6=A_1+2B_1+2E_2+E_1$.[10] To obtain the symmetries of phonon-assisted bound exciton transitions, one should calculate $D_\beta^{ph}\downarrow G_{\mathbf{q}}$. For $G_{\mathbf{q}}=C_{3v}$ ($\mathbf{q}=2a$ or $\mathbf{q}=2b$), we have

$$A_1,B_1\downarrow G_{\mathbf{q}}=a_1, \tag{6a}$$

$$E_1,E_2\downarrow G_{\mathbf{q}}=e, \tag{6b}$$

whereas that for $G_{\mathbf{q}}=C_s$ ($\mathbf{q}=6c$) is

$$A_1,B_1\downarrow G_{\mathbf{q}}=a', \tag{7a}$$

$$E_1,E_2\downarrow G_{\mathbf{q}}=a'+a''. \tag{7b}$$

Next, calculating the direct product $(D_\alpha^{exc}\downarrow G_{\mathbf{q}})\times(D_\beta^{ph}\downarrow G_{\mathbf{q}})$, we determine the selection rules for phonon-assisted transitions of A and B excitons bound to substitutional or interstitial impurities with C_{3v} symmetry and interstitial impurities with C_s symmetry, which are summarized in Table I. For the trivial case of interstitial impurities with C_1 symmetry, the C_1 point group has the only $a(x,y,z)$ irrep and all zero-phonon and phonon-assisted bound exciton transitions are allowed in all polarizations. It should be noted that the substitutional and interstitial impurities occupying $2a$ and $2b$ positions have no differences in symmetry behavior for optical transitions involving only Γ-band states. Therefore, they can not be distinguished on the basis of symmetry only.

We see that optical transitions involving forbidden Γ_5 excitons from the A series become allowed in (x,y) polariza-

tion (equivalent to the σ polarization), when the free exciton is bound to a substitutional impurity and additionally allowed in the z-polarization (π polarization) when E_1 and E_2 phonons are involved in the process. However, the corresponding lines in the spectra are expected to be weak reflecting the coupling strength of excitons to impurities. In turn, the Γ_6 A and B excitons allowed in the (x,y) polarization keep their polarization after binding to the substitutional impurity. The involvement of the A_1 and B_1 phonons does not change the polarization, while the E_1, E_2-phonon-assisted transitions become additionally allowed in the z polarization. For the Γ_1 exciton of the B series, allowed only in the z-polarization, binding to the substitutional impurity as well as the involvement of the A_1 and B_1 phonons does not change the polarization, while the E_1, E_2-phonon-assisted transitions become oppositely (x,y) polarized. It is interesting to notice that the transitions of bound excitons, assisted by the silent B_1 phonon, are nevertheless allowed. This is because for bound excitons the selection rules are determined by the symmetry of the local displacements of the impurity atoms rather than by the symmetry of the extended phonon states of the crystal. These local displacements are equivalent for the A_1 and B_1 phonons, resulting thus in the equivalent selection rules for the respective transitions. For the C_s interstitial impurities, the selection rules practically coincide with those derived for the C_1 impurities—all strong transitions of bound excitons are allowed in all polarizations, it does not matter what is the symmetry of the respective free exciton and phonon.

IV. DISCUSSION

One can check now the correspondence between the theoretical selection rules collected in Table I and experimental data displayed in Figs. 1–3. We omit here any discussion on the polarization properties of the bands of free exciton-polaritons since in addition to the selection rules derived for Γ excitons, their polarization is influenced by a number of specific effects, such as mixing of longitudinal and transverse polariton modes,[16] emergence of the forbidden Γ_5 excitons due to the finite exciton wave vector,[15] and scattering between different polaritonic branches.[17] The lines of donor-bound A excitons $D^0_O X^A$ and $D^0_{Si} X^A$ are strongly σ polarized ($\sim$90%, see Fig. 1). If one makes due allowance for the depolarizing effect of the possible surface roughness of the cleaved surface, it is seen that the intrinsic σ polarization of this lines is close to 100% that implies the C_{3v} site symmetry of the involved impurities. The lines of donor-bound B excitons $D^0_O X^B$ and $D^0_{Si} X^B$ demonstrate a smaller degree of σ polarization ($\sim$70%), which is explained by a certain admixture of $a_1(z)$ excitons (see Table I). This observation is also consistent with the C_{3v} site symmetry of the donors.

The maximum degree of σ polarization within the lines of the LO-phonon replicas shown in Fig. 2 is as low as about 60%. For the C_{3v} impurities, the reduction of the σ polarization is in agreement with the selection rules, which predict a certain contribution of the π polarized emission [$a_1(z)$ term in Table I] for the E_1-phonon-assisted transitions of the bound A excitons. Note that the phonon replicas in Fig. 2 are noticeably broader than the respective zero-phonon lines. The point is that the introduction of impurities breaks the translational symmetry of the lattice and the phonons with $\mathbf{k} \neq 0$ can also participate in phonon-assisted transitions of bound excitons. The selection rules summarized in Table I were written for the Γ phonons with $\mathbf{k}=0$; however, they are valid for all the phonons that, when being subduced on the site symmetry group of the impurity, transform into the mode with the same symmetry (a_1 or e). For example, the $K_1, K_2 \downarrow G_{\mathbf{q}}$ $(\mathbf{q}=2b)=e$; hence, the selection rules, involving these phonons, are like for E_1 and E_2 phonons. However, there are phonon modes, e.g., the K_3 mode, which, when being subduced on the C_{3v} site symmetry group, give both a_1 and e modes. Therefore, all the K_3-phonon-assisted transitions have contributions of both z and (x,y) polarizations. Hence, the degree of polarization can vary within the lines, reflecting the contributions of various phonons. The spectra in Fig. 2 qualitatively represent this behavior. The maximum degree of σ polarization in the spectrum ($\sim$60%) corresponds to the peak attributed to B_1(high)-phonon-assisted transitions of the bound A excitons. According to Table I, this transition is allowed in strict σ polarization. The observed deviation from 100% σ polarization can be due to the strong overlapping with the neighboring line of the E_1(LO)-phonon-assisted transition.

The lines of the E_1(TO)- and E_2(high)-phonon replicas of the two bound A excitons, as shown in Fig. 3, are notably narrower than those of the replica assisted by LO and B_1(high) phonons. Therefore, it is possible to distinguish the peaks relevant to individual phonons and impurities (oxygen and silicon). The reduced degree of σ polarization is specific for all four lines, which is in qualitative agreement with the derived selection rules for any possible position of the impurity atoms. However, quantitatively the two kinds of phonons participate differently, the contribution of the π-polarized emission is much stronger for the transitions assisted by the E_1(TO) phonon. Note also that the polarization properties do not depend on the nature of the involved donor that implies equal site symmetries of the oxygen and silicon atoms.

V. CONCLUSIONS

In conclusion, we have experimentally shown for a high-quality wurtzite GaN crystal that the linear polarization of the emission originating from phonon-assisted transitions of excitons bound on impurities is sensitive to the impurity site symmetry due to the perturbation of the exciton and phonon symmetries. The observed polarization of both zero-phonon and phonon-assisted transitions is consistent with the derived theoretical selection rules, provided both oxygen and silicon impurities occupy positions with the C_{3v} local symmetry.

Furthermore, we observe an emission line, which can be interpreted as a phonon replica of a donor bound exciton, assisted by a silent phonon. The observation of this transition evidences a local character of the exciton-phonon interaction in the case of the impurity bound exciton. In spite of the qualitative agreement between the experimental data and the results of the group-theory analysis, quantitative theoretical consideration of the presented results looks rather difficult.

An approach taking into account all details of the exciton-phonon interaction should be applied to quantify the values of the polarization degree for different participating phonons. We hope that our study will stimulate further theoretical considerations in this field.

ACKNOWLEDGMENTS

This work was supported by the RFBR Grant No. 07-02-00786a. A.A.T. acknowledges support from the Wenner-Gren Foundation, Sweden and Russian Science Support Foundation.

[1] R. Dingle, D. D. Sell, S. E. Stokowski, and M. Ilegems, Phys. Rev. B **4**, 1211 (1971).
[2] W. Y. Liang and A. D. Yoffe, Phys. Rev. Lett. **20**, 59 (1968).
[3] J. J. Hopfield and D. G. Thomas, Phys. Rev. **132**, 563 (1963).
[4] P. Tronc, Yu. E. Kitaev, G. Wang, and M. F. Limonov, Phys. Status Solidi B **210**, 471 (1998).
[5] P. Tronc, Yu. E. Kitaev, A. G. Panfilov, M. F. Limonov, G. Wang, and V. P. Smirnov, Phys. Rev. B **61**, 1999 (2000).
[6] P. Tronc, Yu. E. Kitaev, G. Wang, M. F. Limonov, and G. Neu, Physica B **302**, 291 (2001).
[7] P. P. Paskov, T. Paskova, P. O. Holtz, and B. Monemar, Phys. Rev. B **70**, 035210 (2004).
[8] R. A. Evarestov and V. P. Smirnov, *Site Symmetry in Crystals: Theory and Applications*, Vol. 108, edited by M. Cardona, Springer Series in Solid State Sciences, 2nd ed. (Springer, Berlin, 1997).
[9] B. Monemar, P. P. Paskov, J. P. Bergman, A. A. Toropov, T. V. Shubina, S. Figge, T. Paskova, D. Hommel, A. Usui, M. Iwaya, S. Kamiyama, H. Amano, and I. Akasaki, Mater. Sci. Semicond. Process. **9**, 168 (2006).
[10] V. Yu. Davydov, Yu. E. Kitaev, I. N. Goncharuk, A. N. Smirnov, J. Graul, O. Semchinova, D. Uffmann, M. B. Smirnov, A. P. Mirgorodsky, and R. A. Evarestov, Phys. Rev. B **58**, 12899 (1998).
[11] S. C. Miller and W. F. Love, *Tables of Irreducible Representations of Space Groups and Co-Representations of Magnetic Space Groups* (Pruett, Boulder, 1967).
[12] C. J. Bradley and A. P. Cracknell, *The Mathematical Theory of Symmetry in Solids* (Clarendon, Oxford, 1972).
[13] *International Tables for Crystallography, Vol. A: Space Group Symmetry*, edited by T. Hahn (Reidel, Dordrecht, 1983).
[14] B. Gil and O. Briot, Phys. Rev. B **55**, 2530 (1997); P. Tronc, Yu. E. Kitaev, G. Wang, M. F. Limonov, A. G. Panfilov, and G. Neu, Phys. Status Solidi B **216**, 599 (1999); A. V. Rodina, M. Dietrich, A. Göldner, L. Eckey, A. Hoffmann, Al. L. Efros, M. Rosen, and B. K. Meyer, Phys. Rev. B **64**, 115204 (2001).
[15] D. C. Reynolds, D. C. Look, B. Jogai, A. W. Saxler, S. S. Park, and J. Y. Hahn, Appl. Phys. Lett. **77**, 2879 (2000).
[16] A. A. Toropov, O. V. Nekrutkina, T. V. Shubina, Th. Gruber, C. Kirchner, A. Waag, K. F. Karlsson, P. O. Holtz, and B. Monemar, Phys. Rev. B **69**, 165205 (2004).
[17] T. V. Shubina, T. Paskova, A. A. Toropov, S. V. Ivanov, and B. Monemar, Phys. Rev. B **65**, 075212 (2002).